FERMILAB-PUB-12-573-T
CERN-PH-TH-2012-273

A Higgs Impostor in Low-Scale Technicolor

Estia Eichten[1]*, Kenneth Lane[2]†, and Adam Martin[3,4]‡
[1]Theoretical Physics Group, Fermi National Accelerator Laboratory
P.O. Box 500, Batavia, Illinois 60510
[2]Department of Physics, Boston University
590 Commonwealth Avenue, Boston, Massachusetts 02215
[3]PH-TH Department, CERN
CH-1211 Geneva 23, Switzerland
[4]Department of Physics, University of Notre Dame§
Notre Dame. Indiana 46556

January 28, 2013

Abstract

We propose a "Higgs impostor" model for the 125 GeV boson, X, recently discovered at the LHC. It is a technipion, η_T, with $I^G J^{PC} = 0^- 0^{-+}$ expected in this mass region in low-scale technicolor. Its coupling to pairs of standard-model gauge bosons are dimension-five operators whose strengths are determined within the model. It is easy for the gluon fusion rate $\sigma B(gg \to \eta_T \to \gamma\gamma)$ to agree with the measured one, but $\eta_T \to ZZ^*, WW^*$ are greatly suppressed relative to the standard-model Higgs rates. This is a crucial test of our proposal. In this regard, we assess the most recent data on X decay modes, with a critical discussion of $X \to ZZ^* \to 4\ell$. In our model the η_T mixes almost completely with the isovector π_T^0, giving two similar states, η_L at 125 GeV and η_H higher, possibly in the range 170–190 GeV. Important consequences of this mixing are (1) the only associated production of η_L is via $\rho_T \to W\eta_L$, and this could be sizable; (2) η_H may soon be accessible in $gg \to \eta_H \to \gamma\gamma$; and (3) LSTC phenomenology at the LHC is substantially modified.

*eichten@fnal.gov
†lane@physics.bu.edu
‡adam.martin@cern.ch
§Visiting scholar

1. Introduction

The stunning discovery by ATLAS and CMS of a new boson X at 125 GeV decaying into $\gamma\gamma$ and, at lower significance, ZZ^* and WW^* [1, 2] is widely suspected to be the long-sought Higgs boson of the standard model (SM) of electroweak interactions [3, 4, 5, 6, 7, 8]. It is also widely believed that the collaborations' latest releases of data [9, 10, 11, 12] strongly support this suspicion [13, 14]. However, as emphasized by Wilson (quoted in Ref. [15]) and 't Hooft [16] this explanation for the origin of electroweak symmetry breaking is very unsatisfactory. It is beset by the great problems of naturalness, hierarchy and flavor—the number, masses and mixings of the fermion generations. Notwithstanding this, the discovery clearly puts great pressure on technicolor, the scenario for the Higgs mechanism which needs no Higgs-like boson [17, 15]. This is especially true in low-scale technicolor (LSTC) [18, 19]. As far as we understand, there is no LSTC bound state that mimics H-decays in all these channels and at the rates expected on the basis of the observed $\sigma(pp \to X)B(X \to \gamma\gamma)$.[1,2]

In this paper we propose that $X(125)$ is a state expected in a two-scale model of LSTC and which may be consistent with the data made public so far. This state is a would-be axion, a mixture of neutral isoscalar pseudoscalars occurring in each scale-sector that would be nearly massless if it were not for extended technicolor (ETC) interactions connecting the technifermions of the two scales. We call this particle the $\eta_{_T}$. It has $CP = -1$.[3] As we will see, $\sigma B(pp \to \eta_{_T} \to \gamma\gamma)$ can be larger than the corresponding SM Higgs cross section, and easily match the current experimental observation. In the model we study, there is an unanticipated and interesting possibility: the $\eta_{_T}$ mixes, probably very substantially, with the neutral isovector $\pi^0_{_T}$ expected in LSTC. This results in two states, $\eta_{_L}$ at 125 GeV and a heavier state $\eta_{_H}$ which, we will argue, is likely to be at 170–190 GeV. They have similar production and decay modes, characteristic of both $\eta_{_T}$ and $\pi^0_{_T}$. We shall refer to our Higgs impostor as $\eta_{_T}$ in the absence of large mixing, or as $\eta_{_L}$ if mixing is important.

First, however, we ask: is $X(125)$ a Higgs boson? If analyses of the data in hand, approximately 5 fb^{-1} at 7 TeV and 20 fb^{-1} at 8 TeV, establish that the rates for $pp \to X \to ZZ^*$ and WW^* are in accord with the standard model and that $X \to \tau^+\tau^-$ and $\bar{b}b$ are convincingly seen at Higgsish rates, it will be difficult to resist the conclusion that X is a Higgs boson, perhaps even the SM Higgs boson, H. At this early stage of X-physics

[1] There is a low-lying $I^G J^{PC} = 0^+0^{++}$ state in LSTC with many of the same decays as the standard model H, but its production rate is too small to be the boson observed at the LHC [20]

[2] It is argued by some that walking technicolor or similar models have a light scalar due to their near-conformal invariance being spontaneously broken. This is called the "techni-dilaton". It is also argued that it has Higgs-like couplings to gauge bosons and fermions; see e.g., Refs. [21, 22, 23, 24, 25, 26, 27]. In our view, the existence of such a state is questionable. An interesting paper that discusses the phenomenology of a light dilaton while merely assuming its existence is Ref. [28].

[3] In addition to the dilaton papers cited above, others that have recently suggested a pseudoscalar Higgs impostor in the context of strong electroweak symmetry breaking include Refs. [29, 30, 31, 32, 33, 34, 35]. Unlike our model, most of these do not determine the energy scale and other factors in the dimension-five operators that couple the pseudoscalar to a pair of SM gauge bosons; see Eqs. (29)–(40).

studies, however, there are several possibly statistical peculiarities and discrepancies with the standard model or between the experiments [1, 2, 36, 9, 10, 11, 12]that allow for an alternative explanation. These are discussed in Sec. 2 with special attention to the high mass-resolution process $X \to ZZ^* \to 4\ell$.

In Sec. 3 we present a two-scale model for the $\eta_{_T}$. This model is not unique, but it is simple. Because the $\eta_{_T}$ is a pseudo-Goldstone boson of a chiral symmetry spontaneously broken to a vectorial one, it has $CP = -1$ and all its interactions with a pair of SM gauge bosons are of the nonrenormalizable Wess-Zumino-Witten (WZW) type [37, 38]. In Sec. 4 we discuss mixing of the isoscalar $\eta_{_T}$ with the isovector $\pi^0_{_T}$. This mixing is essentially complete in our model and it may be a general feature of two-scale models with rather widely separated energy scales. This gives two states, $\eta_{_L}$ at 125 GeV and a similar state $\eta_{_H}$ at higher mass. If the dijet excess reported by CDF [39] is real and is described by LSTC [40] then we predict $M_{\eta_{_H}} = 170$–$190\,\text{GeV}$. We urge a search for such a state decaying to two photons. The WZW interactions of our Higgs impostor are determined in Sec. 5 for the unmixed and mixed cases. Compared to the SM Higgs boson, they imply very little $\eta_{_T} \to WW^*$, ZZ^* and vector boson fusion (VBF) of $\eta_{_T}$ via WW and ZZ. There is also little associated production of $\eta_{_T}$ with W or Z *unless* it mixes appreciably with $\pi^0_{_T}$. In that case, and assuming the validity of the CDF Wjj data, $\rho^\pm_{_T} \to \eta_{_L} W^\pm$ readily occurs, but *not* $\rho^0_{_T} \to \eta_{_L} Z$. Decays of $\eta_{_L}$ are dominated by $\eta_{_T} \to gg$ and, so, $\eta_{_L}$ decays nearly 100% of the time to gg. This may pollute and alter the SM $WW/WZ \to \ell\nu jj$ signal *and* the CDF dijet excess. We also discuss $\eta_{_T}$ couplings to fermion pairs; these are induced by ETC and are, therefore, rather uncertain.

The phenomenology of $\eta_{_L}$ is presented in Sec. 6. In detail, it is specific to our two-scale model, but the general features, especially those dictated by the WZW interactions, hold in any such model. In particular: (1) By far, the dominant $\eta_{_L}$-production mechanism is via gluon fusion. Generally, we find that $\sigma(gg \to \eta_{_L}) > \sigma(gg \to H)$. Obtaining the correct $\sigma B(gg \to \eta_{_L} \to \gamma\gamma)$ rate is then due to a fortuitous (but ubiquitous) cancellation among the terms in the $\gamma\gamma$ amplitude. (2) As noted, the branching ratios $B(\eta_{_L} \to ZZ^*, WW^* \to$ leptons) are extremely small. Therefore, according to our model's framework, what has been observed by CMS and ATLAS must be background. The current experimental situation, which we critique in Sec. 2, still allows this possibility. (3) The branching ratios of $\eta_{_L}$ to $\tau^+\tau^-$ and $\bar{b}b$ depend on the unknown couplings of $\eta_{_T}$ and $\pi^0_{_T}$ to these fermions in the underlying ETC model. We fix them to be consistent with current data. In Sec. 7 we summarize the consequences of $\eta_{_T}$-$\pi^0_{_T}$ mixing on the low-scale $\rho_{_T}$ phenomenology at the LHC. These are dramatic if the mixing is as large as we find in Sec. 4, and we expect it to be more difficult to detect the signatures we discussed in Ref. [41].

2. X-Decay Data in 2012

The new boson X is widely referred to as being "Higgs-like" because it *appears* to have been observed in several of the experimentally most accessible decay channels of the SM

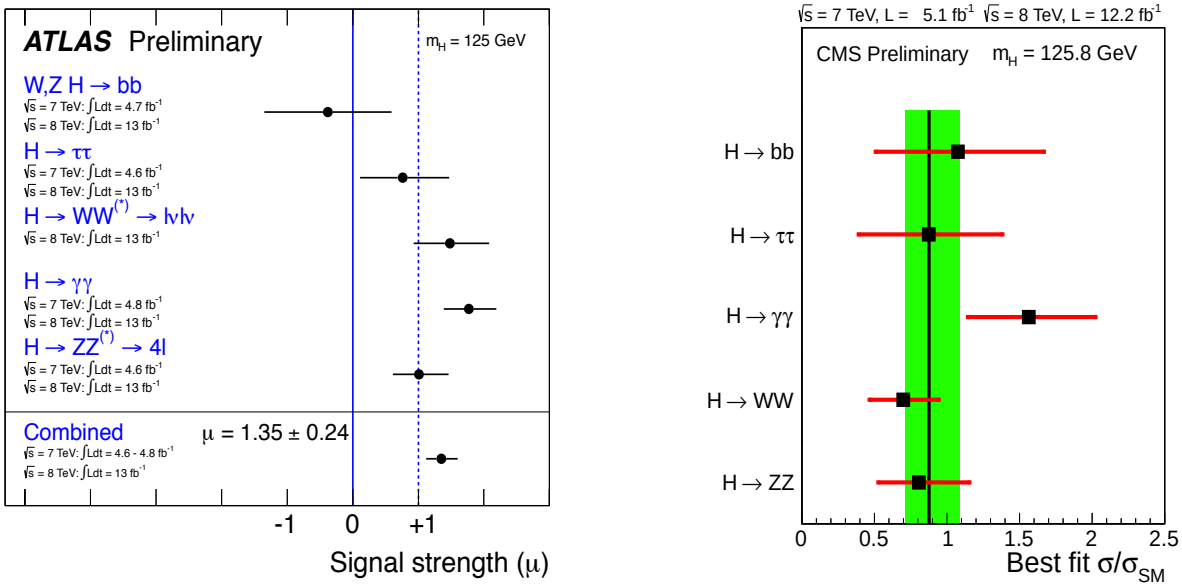

Figure 1: The signal strengths $\mu(F) = \sigma B(pp \to X \to F)/\sigma B(pp \to H \to F)$ determined by ATLAS as of December 2012 [11] (left) and CMS as of November 2012 [9] (right) for luminosities of about $5\,\text{fb}^{-1}$ at 7 TeV and 12–13 fb^{-1} at 8 TeV (except that CMS's $\gamma\gamma$ data at 8 TeV is based on only $5\,\text{fb}^{-1}$).

Higgs boson, namely $\gamma\gamma$, $ZZ^* \to \ell^+\ell^-\ell^+\ell^-$ ($\ell = e$ and/or μ), $WW^* \to \ell^+\nu\ell^-\nu$, $\tau^+\tau^-$ and $WX \to \ell\nu\bar{b}b$. Furthermore, σB for these channels are roughly consistent with those predicted for a standard model Higgs of mass 125 GeV. We say "appears" because, as we now discuss, the evidence for some of these decay channels is rather weak and, we believe, the important $ZZ^* \to 4\ell$ channel is still dominated by statistics.

1. ATLAS and CMS obtained the $\mu(\gamma\gamma) \equiv \sigma B(pp \to X \to \gamma\gamma)/\sigma B(pp \to H \to \gamma\gamma) = 1.8 \pm 0.7$ and 1.6 ± 0.4 for the SM Higgs H. This is the most compelling evidence for production of the new particle X and for its interpretation as a Higgs boson. This "signal strength" and others, $\mu(F)$ for final state F, are summarized in Fig. 1. The $\mu(\gamma\gamma)$ is dominated by events with no tagged forward jet (untagged), though there is some contribution from events with one or more tagged forward jet — so-called vector-boson fusion or VBF tag, though there is no evidence that the tagged jet is associated with WW or ZZ fusion of X, and it may have arisen from gluon (gg) fusion. Note that the CMS $\gamma\gamma$ data has not been updated since July 2012.

2. Despite its low rate, the channel $X \to ZZ^* \to 4\ell$ is very important because of its excellent mass resolution. Because of this, it has the highest significance after $\gamma\gamma$. Nevertheless, we believe that this ZZ^* (and $Z\gamma^*$) data is still subject to rather large statistical fluctuations and does not yet provide the evidence for a Higgs-boson interpretation of X commonly attributed to it as, e.g., in Refs. [13, 14].

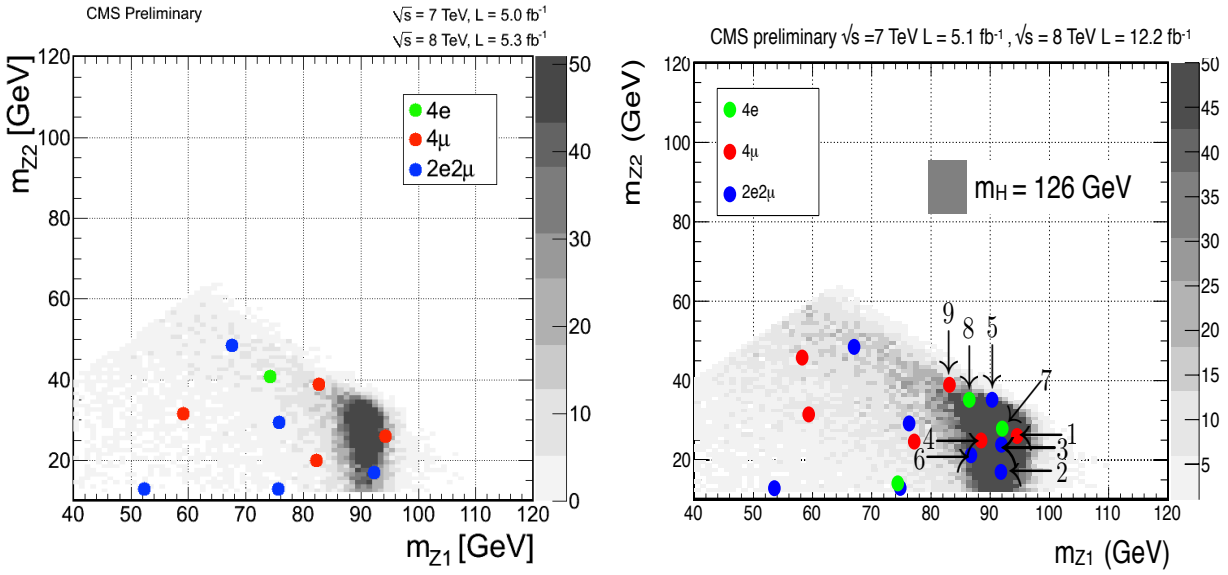

Figure 2: The Dalitz plot of high vs. low dilepton mass, M_{Z1} vs. M_{Z2} in the four-lepton invariant mass region $120\,\text{GeV} < M_{4\ell} < 130\,\text{GeV}$ from CMS in July at ICHEP-2012 [36] (left) and November 2012 [42] (right). We have numbered "signal-like" events as described in the text.

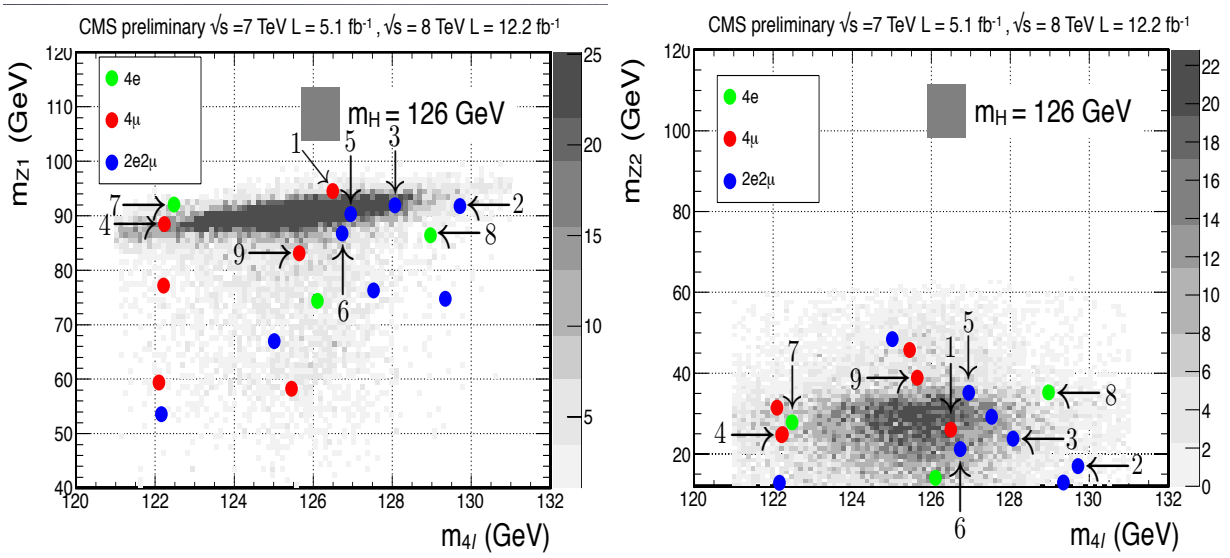

Figure 3: The Dalitz plot of M_{Z1} (left) and M_{Z2} (right) vs. $M_{4\ell}$ in the region $120\,\text{GeV} < M_{4\ell} < 130\,\text{GeV}$ from CMS [42]. The numbering of events is the same as in Fig. 2 and is described in the text.

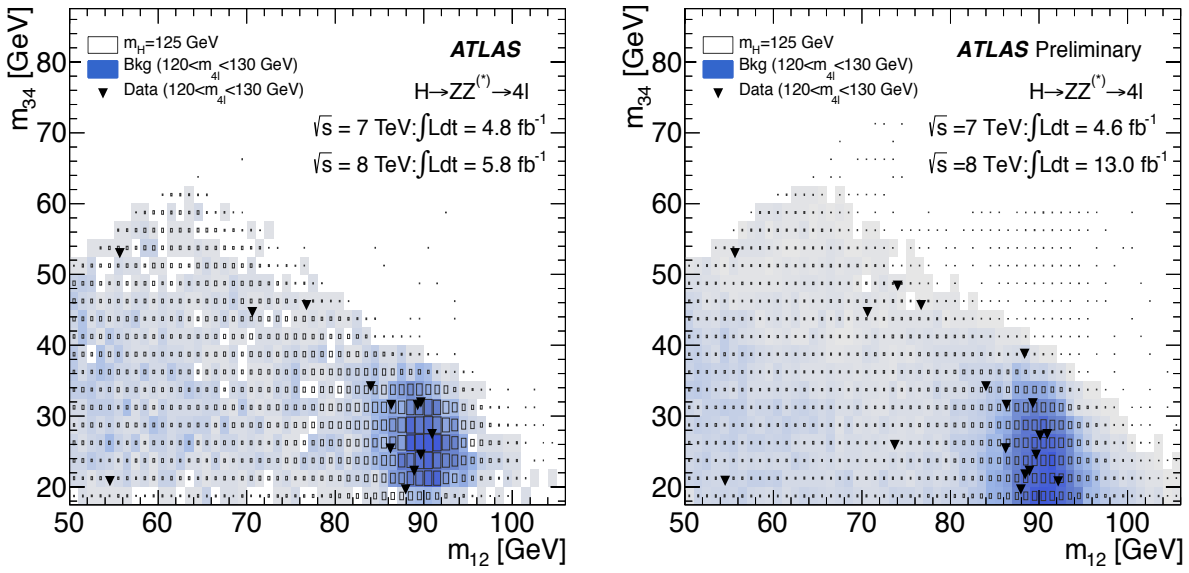

Figure 4: The Dalitz plot of high vs. low dilepton mass, M_{12} vs. M_{34}, in the region $120\,\text{GeV} < M_{4\ell} < 130\,\text{GeV}$ from ATLAS in July 2012 [1] (left) and December 2012 [12] (right).

In the CMS data released in July, there were ten events, including an expected background of three, with four-lepton invariant mass $120\,\text{GeV} < M_{4\ell} < 130\,\text{GeV}$. As seen on the left in Fig. 2, only two (or, at most, four) of the events in CMS's plot of M_{Z1} vs. M_{Z2} appear to have a real Z-boson, those with $85\,\text{GeV} \lesssim M_{Z1} \lesssim 95\,\text{GeV}$, whereas 70–80% of ZZ^* in this mass range are expected to have a real Z. This data was based on two sets of about $5\,\text{fb}^{-1}$ each taken at $\sqrt{s} = 7$ and $8\,\text{TeV}$. CMS updated its ZZ^*/γ^* data in November, with a total of $12.2\,\text{fb}^{-1}$ at $8\,\text{TeV}$. This data has 17 events with an expected background of six in $M_{4\ell} = 120$–$130\,\text{GeV}$. The new M_{Z1} vs. M_{Z2} plot has 8–9 real Z's, i.e., essentially all of the new events are in the dark signal region; see Fig. 2.[4] Statistically, CMS was unlucky in July or unlucky in November.

A closer look at the CMS ZZ^* signal data makes it even less convincing. In Fig. 2 we numbered the 8 or 9 "golden" events with a real Z. Numbers 1 and 2 are the original two golden events. In Fig. 3 all the events, including the ones we numbered, are shown in two plots, M_{Z1} vs. $M_{4\ell}$ and M_{Z2} vs. $M_{4\ell}$, from [42]. In M_{Z1} vs. $M_{4\ell}$, only events 3 and 5 are in the Monte Carlo signal's dark region. Events 1,4,6 are on the lighter edges of this region. In M_{Z2} vs. $M_{4\ell}$, only events 1 and 6 are the dark part of the signal region; marginally, events 3,5,7 are may be included. Thus, *no* real-Z event is in the dark signal region of all three plots. More generously, only the four real-Z events 1,3,5,6 are in the signal region of all three plots. This is about 1/2 the expected

[4]It is unclear to us why the M_{Z1}-width of this region almost doubled between July and November. That did not happen with the ATLAS data in Fig. 4.

number of $H \to ZZ^* \to 4\ell$ signal events.

The ATLAS ZZ^*/γ^* data released in July [1] and in December [12] are shown in Fig. 4. Note first that the ATLAS plots reveal that the region of maximum $H \to ZZ^*$ production is right where the background peaks, usually a cause for concern. ATLAS's July data, based on $4.8\,\text{fb}^{-1}$ at 7 TeV and $5.8\,\text{fb}^{-1}$ at 8 TeV are more Higgs-like than the July CMS data: there are 13 events with $120\,\text{GeV} < M_{4\ell} < 130\,\text{GeV}$, of which 8–9 appear to have a real Z and are in the Higgs signal region of the Monte Carlo. The data released in December included $13\,\text{fb}^{-1}$ at 8 TeV. They have 18 events, but only two new ones are in the Higgs signal region. (It appears that one July event's M_{34} decreased from about 32 GeV to 28 GeV.) There are ten apparently real-Z events in the signal region on the right in Fig. 4. We analyzed these as we did the nine CMS events. We found that only two are in the signal region of all three plots. A more generous definition of the $H \to ZZ^*$ regions yields four in all three plots. As for CMS, it appears that statistics are at work here.

ATLAS [12] and CMS [43] have also published angular distributions or discriminants based on their $ZZ^* \to 4\ell$ events that are intended to differentiate between $J^P = 0^+$ and 0^- for X(125). Given our arguments that neither experiment's ZZ^* data yet has the statistical strength required for a demonstration of $H \to ZZ^*$, we do not believe that a convincing spin-parity analysis can be made from this data set. This view is strengthened by the actual angular distribution data in Fig. 18 or Ref. [12] and Fig. 2 of Ref. [43]. They appear incapable of distinguishing the two cases.

3. The channel $X \to WW^* \to \ell\nu\ell\nu$ channel is also important, but not nearly so much as $ZZ^* \to 4\ell$ because of the large missing energy and lack of a well-defined discrete mass for its source. The ATLAS and CMS data in July and December were mildly inconsistent. The latest quoted signal strengths for this channel are $\mu(WW^*) = 1.5 \pm 0.6$ for ATLAS [11] and 0.7 ± 0.2 for CMS [10]

4. The decay $H \to \tau^+\tau^-$ is best sought in the associated production modes $WH \to \ell\nu\tau\tau$ and $ZH \to \ell^+\ell^-\tau\tau$ because of very large background from $Z \to \tau^+\tau^-$. CMS reported $\mu(\tau^+\tau^-) = 0.0 \pm 0.8$ in July and 0.9 ± 0.5 in November. This result is dominated by $\tau^+\tau^-$ produced with zero or one jet (gg and/or VB fusion), but with rather large errors; the result for W/ZX associated production is consistent, but with very large error. ATLAS first reported on this mode in November, with $\mu(\tau^+\tau^-) = 0.8 \pm 0.7$. In short, the evidence for $X \to \tau^+\tau^-$ is weak, but this is not surprising given the difficulty of detecting it.

5. In July, neither ATLAS nor CMS reported observing the associated production mode $WX \to \ell\nu\bar{b}b$, but this too is not surprising given the large backgrounds to this signal at the LHC. The CDF and DØ experiments combined their search for $\bar{p}p \to WH$, ZH with $H \to \bar{b}b$ and claimed a signal consistent with $X(125)$ at the $3.1\,\sigma$ level [44]. This

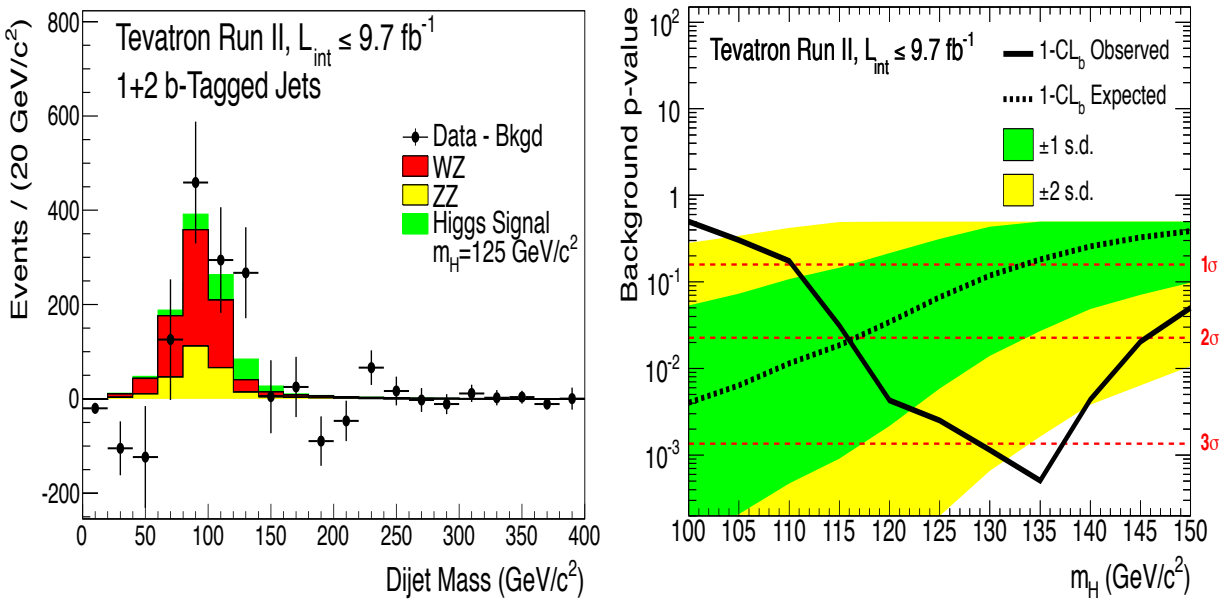

Figure 5: CDF and DØ data on $\bar{p}p \to W\bar{b}b$ with $M_{\bar{b}b}$ in the 125 GeV region [44]. See the text for comments.

was surprising considering that $S/B < 1\%$ for the samples used for this channel [45]. Moreover, as Fig. 5 shows, the broad mass peak is not a convincing fit to $M_H = 125\,\text{GeV}$ and its significance is greatest at $M_{\bar{b}b} = 135\,\text{GeV}$.[5] In November, CMS reported $\mu(\bar{b}b) = 1.1 \pm 0.6$, entirely from $WX \to \ell\nu\bar{b}b$ [9]. ATLAS still has no signal, with $\mu(\bar{b}b) = -0.4 \pm 1.0$. [11].

Of course, these fluctuations and disagreements may disappear with more data. For now, they are tantalizing, and alternative interpretations of $X(125)$ are worth exploring.

3. A Two-Scale Model for the η_T

The technipion η_T is a pseudo-Goldstone boson that must occur in LSTC models [18]. It was referred to as $\pi_T^{0\prime}$ in previous papers, e.g., Ref. [19], which also contains a more complete description of LSTC. Since η_T is a pseudoscalar and decays to two photons, it has $CP = -1$. Therefore, it has no renormalizable couplings to a pair of SM gauge bosons. Its main production mechanism, therefore, must be via gluon (gg) fusion. This requires that η_T be composed, at least in part, of technifermions carrying ordinary $SU(3)_C$ color.[6] In LSTC,

[5]The CDF-DØ paper does not make clear what correction was made for lost neutrinos and muons in the 40% of b-semileptonic decays in $\bar{b}b$ states. Therefore, the actual $\bar{b}b$ mass peak might be even higher, closer to 145–150 GeV [39].

[6]The top quark cannot couple strongly to η_T nor any other π_T because, in ETC models with fermion-bilinear anomalous dimension $\gamma_m \leq 1$ [46], m_t must arise from some other strong interaction, such as

we usually assume that the lightest (lowest-scale) technifermions are $SU(3)_C$-singlets, and we make that assumption here. Thus, for an $\eta_T gg$ interaction to occur, the higher-scale technifermions must be colored.[7] To describe this, we adopt the following two-scale model:

$$\begin{aligned}
\text{Scale 1:}\quad T_1 \equiv \begin{pmatrix} U_1 \\ D_1 \end{pmatrix} &= \begin{cases} T_{1L} & = (\square, 1, 2)_{Y_1} \\ U_{1R} & = (\square, 1, 1)_{Q_{U1}} \\ D_{1R} & = (\square, 1, 1)_{Q_{D1}} \end{cases} \\
\text{Scale 2:}\quad T_2 \equiv \begin{pmatrix} U_2 \\ D_2 \end{pmatrix} &= \begin{cases} T_{2L} & = (\begin{smallmatrix}\square\\\square\end{smallmatrix}, \square, 2)_{Y_2} \\ U_{2R} & = (\begin{smallmatrix}\square\\\square\end{smallmatrix}, \square, 1)_{Q_{U2}} \\ D_{2R} & = (\begin{smallmatrix}\square\\\square\end{smallmatrix}, \square, 1)_{Q_{D2}} \end{cases}
\end{aligned} \tag{1}$$

under $(SU(N_{TC}), SU(3)_C, SU(2))_{U(1)}$. Here, $Y_i = \frac{1}{2}(Q_{Ui} + Q_{Di})$.

We emphasize that this model's purpose is to illustrate our LSTC proposal to account for the $X(125)$ data. Different TC representations and/or input parameters (N_{TC}, etc.) could give quantitatively different results, and more data may require a refinement of the model. Nevertheless, we believe the model's general features—the interactions η_T has with ordinary matter and the typical strength of these interactions—will survive as long as the viability of an LSTC impostor of $X(125)$ does.

When the technifermions T_1 and T_2 condense, there are a number of Goldstone bosons (all but three of which must get mass from ETC interactions [49]) including two color-singlets with $I^G J^{PC} = 0^+0^{-+}$ we call η_1 and η_2. These couple to the $U(1)$ axial vector currents $j_{i,5\mu} = \frac{1}{2}\bar{T}_i\gamma_\mu\gamma_5 T_i$ as

$$\langle\Omega|j_{1,5\mu}|\eta_1(p)\rangle = iF_1 p_\mu, \qquad \langle\Omega|j_{2,5\mu}|\eta_2(p)\rangle = i\sqrt{3}F_2 p_\mu, \tag{2}$$

where F_1 and F_2 are the basic (canonically normalized) π_T decay constants of scales 1 and 2. They are related to the weak decay constant $F_\pi \equiv v = 246\,\text{GeV}$ and the LSTC mixing angle parameter $\sin\chi$ [50, 19] by

$$F_\pi = \sqrt{F_1^2 + 3F_2^2}, \qquad F_1 = F_\pi \sin\chi, \quad \sqrt{3}F_2 = F_\pi\cos\chi\,. \tag{3}$$

A recent search by CMS for $\rho_T \to WZ \to 3\ell\nu$ put a 95% upper limit of about 20 fb on its cross section at $M_{\rho_T} = 275$–$290\,\text{GeV}$ and $M_{\pi_T} > 140\,\text{GeV}$ [48]. This requires $\sin\chi \lesssim 0.30$ for the LSTC model with these masses [41]. While this bound is relevant for the case of little or no η_T-π_T^0 mixing, sizable mixing probably weakens it; see Sec. 7.

The $U(1)$ currents have divergences with TC-gluon anomalous terms and other explicit breaking:

$$\partial^\mu j_{i,5\mu} = -\frac{g_{TC}^2}{16\pi^2} N_i G_{T,\mu\nu}\widetilde{G}_T^{\mu\nu} + i[\mathcal{Q}_{i,5}, \mathcal{H}_{ETC}] + \cdots\,, \tag{4}$$

topcolor [47].

[7] An alternative in which the lightest-scale technifermions are colored might be interesting, but we shall not consider it here. As Eq. (3) indicates, this tends to imply a larger value of the LSTC parameter $\sin\chi$ in Eq. (3) and that is disfavored experimentally [48, 41].

where $\widetilde{G}_{T,\mu\nu} = \frac{1}{2}\epsilon_{\mu\nu\lambda\rho}G_T^{\lambda\rho}$, $\mathcal{Q}_{i,5} = \int d^3x\, j_{i,50}$, $\mathcal{H}_{ETC}$ is a 4-technifermion interaction involving T_1 and T_2, and the ellipses are $SU(3)_C \otimes SU(2) \otimes U(1)$ anomalous divergences that will be specified in Sec. 5. In Eq.(4) the numerical factors are $N_i = 2T(R_{TC,i})d(R_{C,i})$, where the factor 2 is for isodoublet technifermions, $T(R_{TC})$ is the trace of a square of generators for TC-representation R ($= \frac{1}{2}$ for fundamentals of $SU(N_{TC})$) and $d(R_C)$ is the dimension of the $SU(3)_C$ representation. In the model of Eq. (1),

$$N_1 = 2 \cdot \tfrac{1}{2} \cdot 1 = 1, \quad N_2 = 2 \cdot \tfrac{1}{2}(N_{TC} - 2) \cdot 3 = 3(N_{TC} - 2)\,. \tag{5}$$

The current $j'_{5\mu} = j_{1,5\mu} + j_{2,5\mu}$ is conserved by ETC interactions (see Sec. 4) but not by the TC anomaly:

$$\partial^\mu j'_{5\mu} = -\frac{g_{TC}^2}{16\pi^2}(N_1 + N_2)G_{T,\mu\nu}\widetilde{G}_T^{\mu\nu} + \cdots\,. \tag{6}$$

It couples to a linear combination η'_T of η_1 and η_2 which gets its mass mainly from TC instantons and is heavy. The orthogonal linear combination is the $\eta_{_T}$ and its mass arises from $\mathcal{H}_{ETC}$. It couples to the TC-anomaly-free current

$$\begin{aligned} j_{5\mu} &= N_2 j_{1,5\mu} - N_1 j_{2,5\mu} && (7)\\ \partial^\mu j_{5\mu} &= i[N_2\mathcal{Q}_{1,5} - N_1\mathcal{Q}_{2,5}, \mathcal{H}_{ETC}] + \cdots = i(N_1 + N_2)[\mathcal{Q}_{1,5}, \mathcal{H}_{ETC}] + \cdots\,. && (8)\end{aligned}$$

Let us write

$$\begin{aligned} |\eta'_T\rangle &= |\eta_1\rangle \sin\eta + |\eta_2\rangle \cos\eta \\ |\eta_{_T}\rangle &= |\eta_1\rangle \cos\eta - |\eta_2\rangle \sin\eta\,. \end{aligned} \tag{9}$$

The mixing angle η is determined by noting that, unless the matrix element $\langle\Omega|j_{5\mu}|\eta'_T\rangle = 0$ in the limit $\mathcal{H}_{ETC} \to 0$, then $M_{\eta'_{_T}} \cong 0$ since this current is TC-anomaly free. This yields

$$\sin\eta = \frac{\sqrt{3}N_1F_2}{F_{\eta_T}}, \quad \cos\eta = \frac{N_2F_1}{F_{\eta_T}}, \qquad \text{where} \quad F_{\eta_T} = \sqrt{N_2^2F_1^2 + 3N_1^2F_2^2}\,. \tag{10}$$

Noting that

$$F_{\eta_T} = \sqrt{N_2^2\sin^2\chi + N_1^2\cos^2\chi}\,F_\pi\,, \tag{11}$$

we have

$$\sin\eta = \frac{N_1\cos\chi}{\sqrt{N_2^2\sin^2\chi + N_1^2\cos^2\chi}}, \quad \cos\eta = \frac{N_2\sin\chi}{\sqrt{N_2^2\sin^2\chi + N_1^2\cos^2\chi}}\,. \tag{12}$$

For $N_{TC} = 4$ and $\sin\chi = 0.3$, we have $N_1 = 1$, $N_2 = 6$, $\sin\eta = 0.468$, $\cos\eta = 0.884$, and $F_{\eta_T} = 501\,\text{GeV}$ is the normalized decay constant of the $\eta_{_T}$.

4. η_T-π_T^0 Mixing

The state η_T discussed in Sec. 3 generally is not a mass eigenstate. In the model we have presented and in similar ones, the ETC interactions that give it mass also mix it with the neutral isovector technipion π_T^0 discussed in Refs. [40, 41]. This effects not only η_T phenomenology but, as we discuss in Sec. 7, the LSTC description of the CDF dijet excess observed near $M_{jj} = 150\,\mathrm{GeV}$ in Wjj production [39, 51]. The ETC interactions of T_1 and T_2 must be $SU(N_{TC}) \otimes SU(3)_C \otimes SU(2) \otimes U(1)$ invariant. For our model they have the following form at energies far below the masses $M_{1,2,3}$ of ETC gauge bosons:

$$\begin{aligned} \mathcal{H}_{ETC} &= \frac{g_{ETC}^2}{M_1^2}\,\bar{T}_{1L}\gamma^\mu T_{1L}\bar{T}_{1R}\gamma_\mu(a_1 + b_1\tau_3)T_{1R} \\ &+ \frac{g_{ETC}^2}{M_2^2}\,\left(\bar{T}_{1L}\gamma^\mu T_{2L}\bar{T}_{2R}\gamma_\mu(a_2 + b_2\tau_3)T_{1R} + \mathrm{h.c.}\right) \\ &+ \frac{g_{ETC}^2}{M_3^2}\,\bar{T}_{2L}\gamma^\mu T_{2L}\bar{T}_{2R}\gamma_\mu(a_3 + b_2\tau_3)T_{2R}\,. \end{aligned} \tag{13}$$

The $SU(N_{TC}) \otimes SU(3)_C$ indices of these interactions are suppressed, but the structure of the middle term, e.g., is

$$\bar{T}_{1L}^{\alpha}\gamma^\mu T_{2L}^{[\alpha\beta],k}\bar{T}_{2R}^{[\beta\gamma],k}\gamma_\mu(a_2 + b_2\tau_3)T_{1R}^{\gamma}\,, \tag{14}$$

where $\alpha, \beta, \gamma = 1, 2, \ldots, N_{TC}$ are $SU(N_{TC})$ indices with $[\alpha\beta] = -[\beta\alpha]$ and $k = 1, 2, 3$ is an $SU(3)_C$ index. The $SU(2)_R$ violation in the b-terms is necessary to split up from down-fermions. We expect $a_i, |b_i| = \mathcal{O}(1)$ with $a_i > 0$ while b_i may have either sign.

To a very good approximation, the masses and mixing of the technipions $\pi_T^\pm$, π_T^0 and η_T come entirely from the $\bar{T}_1 T_2 \bar{T}_2 T_1$ terms, and they are determined as follows: In the absence of η_T-π_T^0 mixing, the mass eigenstates $|\pi_T^a\rangle$ $(a = 1, 2, 3)$ are the linear combination

$$|\pi_T^a\rangle = \cos\chi|\pi_1^a\rangle - \sin\chi|\pi_2^a\rangle, \tag{15}$$

where $|\pi_{1,2}^a\rangle$ are the scale-1,2 color-singlet technipions. The mixing angle χ was defined in Eq. (3), with $\sin\chi > 0$. The orthogonal combinations are the three Goldstone components of the electroweak bosons, $|W_L^a\rangle$. The state $|\pi_T^a\rangle$ does not couple to the conserved electroweak axial current $j_{5\mu}^{a,EW} = j_{1,5\mu}^a + j_{2,5\mu}^a + \cdots$, where $j_{i,5\mu}^a = \frac{1}{2}\bar{T}_i\gamma_\mu\gamma_5\tau_a T_i$; if it did, $M_{\pi_T} = 0$. The π_T^a current we will use for calculating M_{π_T} is

$$j_{5\mu}^a = j_{1,5\mu}^a \cot\chi - j_{2,5\mu}^a \tan\chi\,. \tag{16}$$

This current couples to π_T in Eq. (15) with strength F_π,

$$\langle\Omega|j_{5\mu}^a|\pi_T^b(p)\rangle = iF_\pi p_\mu\delta_{ab}\,, \tag{17}$$

but not to the orthogonal combination, the erstwhile Goldstone bosons that are the longitudinally-polarized $W^\pm$ and Z. Then, with $\mathcal{Q}_5^a = \int d^3x\, j_{50}^a$ for $a = 1, 2, 3$, and using isospin and parity

invariance of the vacuum state $|\Omega\rangle$, we obtain [52]

$$\begin{aligned} F_\pi^2 M_{\pi_T}^2 &= i^2 \langle\Omega|[\mathcal{Q}_5^a,[\mathcal{Q}_5^a,\mathcal{H}_{ETC}]]|\Omega\rangle \\ &= \frac{i^2 a_2 g_{ETC}^2}{2M_2^2 \sin^2\chi\cos^2\chi}\langle\Omega|\left[\bar{T}_{1L}\gamma^\mu\tau_a T_{2L}\bar{T}_{2R}\gamma_\mu\tau_a T_{1R} + \bar{T}_{1L}\gamma^\mu T_{2L}\bar{T}_{2R}\gamma_\mu T_{1R} + \text{h.c.}\right]|\Omega\rangle \\ &= \frac{2i^2 a_2 g_{ETC}^2}{M_2^2 \sin^2\chi\cos^2\chi}\langle\Omega|\left[\bar{T}_{1L}\gamma^\mu T_{2L}\bar{T}_{2R}\gamma_\mu T_{1R}\right]|\Omega\rangle\,, \end{aligned} \tag{18}$$

Similarly, with $\mathcal{Q}_5 = N_2\mathcal{Q}_{1,5} - N_1\mathcal{Q}_{2,5}$, we get

$$F_{\eta_T}^2 M_{\eta_T}^2 = \left[(N_1+N_2)\sin\chi\cos\chi\, F_\pi M_{\pi_T}\right]^2 \tag{19}$$

$$F_\pi F_{\eta_T} M_{\eta_T\pi_T^0}^2 = (b_2/a_2)(N_1+N_2)\sin\chi\cos\chi\, F_\pi^2 M_{\pi_T}^2\,. \tag{20}$$

$$\tag{21}$$

Then, using Eq. (11) for F_{η_T},

$$\left(\frac{M_{\eta_T}}{M_{\pi_T}}\right)^2 = \frac{((N_1+N_2)\sin\chi\cos\chi)^2}{N_1^2 + (N_2^2-N_1^2)\sin^2\chi} = 0.967\,(0.998)\,, \tag{22}$$

$$\left(\frac{M_{\eta_T\pi_T^0}}{M_{\pi_T}}\right)^2 = \frac{b_2}{a_2}\left(\frac{M_{\eta_T}}{M_{\pi_T}}\right)^2. \tag{23}$$

Here, M_{π_T} is the mass of the charged $\pi_T^\pm$, which is unaffected by the $|\Delta I| = 1$ isospin breaking in $\mathcal{H}_{ETC}$. The numerical values in Eq. (22) are for $\sin\chi = 0.30$ and $N_{TC} = 4\,(6)$. They will be close to one when $(N_2\sin\chi)^2 \gg N_1^2$ and $\sin^2\chi \ll 1$, as it is here.

Thus, in two-scale models like the one presented here, we have the surprising result that the mass eigenstates are nearly 50-50 admixtures of the neutral isoscalar and isovector technipions,

$$\begin{aligned} |\eta_{_L}\rangle &\cong \sqrt{\tfrac{1}{2}}\left(|\eta_T\rangle - \text{sgn}(b_2)\,\pi_T^0\rangle\right), \\ |\eta_{_H}\rangle &\cong \sqrt{\tfrac{1}{2}}\left(|\eta_T\rangle + \text{sgn}(b_2)\,\pi_T^0\rangle\right), \end{aligned} \tag{24}$$

with masses

$$M_{\eta_{_L}} \cong M_{\pi_T}\sqrt{1-|b_2|/a_2}, \quad M_{\eta_{_H}} \cong M_{\pi_T}\sqrt{1+|b_2|/a_2}. \tag{25}$$

How do we determine the mass of $\eta_{_H}$? One way is this: In recent work [40, 41] we ascribed the CDF dijet mass excess near 150 GeV [39, 51] to the production and decay of the lightest isovector technipions, produced in the LSTC process $\rho_T \to W\pi_T \to \ell\nu jj$. In the present framework, we assume that what CDF saw was $\rho_T^0 \to W^\pm\pi_T^\mp$, with $M_{\pi_T^\pm} = 150$–$160\,\text{GeV}$. The π_T^0 is now part of the mixed-state $\eta_{_L}$, our Higgs impostor, observed by ATLAS and CMS with mass 125 GeV. Then, from Eq. (25), $M_{\eta_{_H}} = 170$–$190\,\text{GeV}$. In Sec. 7, we will see how this interpretation alters LSTC phenomenology at the LHC.[8] This rather precise

[8] We estimate that the Tevatron rate for $W^\pm\pi_T^\mp$ production is about 2.4 pb, essentially the same as our prediction of the total $W\pi_T$ rate in Ref. [40]. This estimate is rough because the PYTHIA code [53] does not properly describe the model with η_T-π_T^0 mixing; see Sec. 7.

prediction for M_{η_H} is satisfying, but it does rely on our description of the CDF excess. If we gave up that description, we would still expect that the η_H—a pseudo-Goldstone boson composed mainly of lighter scale technifermions—would not be very much heavier than η_L. This is clear from Eqs. (25) so long as $|b_2|/a_2$ is not close to one. The converse expectation is also likely true: If $X(125)$ is to be interpreted as an η_T of low-scale technicolor, then there are other technihadron states nearby, and they should be accessible in hadron collider experiments.

5. η_T and π_T^0 Interactions

The couplings between the CP-odd η_T and a pair of SM gauge bosons or SM fermion-antifermion pairs ($\bar{f}f$) are given by

$$\begin{aligned}\mathcal{L}_{\eta_T} &= \frac{\eta_T}{F_{\eta_T}}\partial^\mu j_{5\mu} \equiv \frac{\eta_T}{F_{\eta_T}}\partial^\mu \left(N_2 j_{1,5\mu} - N_1 j_{2,5\mu}\right) \\ &= \text{SM gauge boson anomaly terms} + i[\mathcal{Q}_5, \mathcal{H}_{ETC}]\,. \end{aligned} \tag{26}$$

A similar expression holds for π_T^0 with $F_{\pi_T} \equiv F_\pi$.

The anomaly terms are obtained as was the gauged WZW interaction in Refs [37, 38]. For chiral gauge groups, the simplest way to calculate them is to expand the WZW term to linear order in the technipion fields using a nonlinear-sigma formulation of our model,

$$\Sigma_1 = \exp\left(\frac{2i\boldsymbol{\pi}_1}{F_1}\right), \qquad \Sigma_2 = \exp\left(\frac{2i\boldsymbol{\pi}_2}{\sqrt{3}F_2}\right), \tag{27}$$

with covariant derivative $D_\mu\Sigma_i = \partial_\mu\Sigma_i - i\mathcal{A}_L\Sigma_i + i\Sigma_i\mathcal{A}_R$ where $\mathcal{A}_L = \frac{1}{2}(gW_\mu^a\tau_a + g'Y_i\,B_\mu\tau_0)$ and $\mathcal{A}_R = \frac{1}{2}g'B_\mu(\tau_3 + Y_i\tau_0)$; $\boldsymbol{\pi}_i = \frac{1}{2}(\pi_i^a\tau_a + \eta_i\tau_0)$, with $\tau_0 = \mathbf{1}_2$ and F_1, F_2 are the scale–1,2 technipion decay constants defined earlier. Applying this setup to Eq. (69) of Ref. [54], each techni-sector contributes a WZW term weighted by a coefficient that depends on the number of degrees of freedom in that sector. The total WZW interaction is then $\mathcal{L}_{WZW} = \mathcal{L}_{WZW,1} + \mathcal{L}_{WZW,2}$. For η_T, π_T interactions involving vectorial gauge groups, such as $\eta_T \to \gamma\gamma$ or $\eta_T \to gg$, the WZW result has the familiar form,

$$\partial^\mu j_{i,5\mu} = -\frac{g_A^2}{32\pi^2}\mathrm{Tr}\left(\tau_0\left\{t_{i,a}^A, t_{i,b}^A\right\}\right) G_{\mu\nu}^{Aa}\widetilde{G}^{Ab,\mu\nu}\,, \tag{28}$$

where $t_{i,a}^A$ is the a-th generator of technifermion doublet T_i in gauge group A. The corresponding expression for $\partial^\mu j_{5\mu}^3$ has the trace $\mathrm{Tr}(\tau_3\{t_{i,a}^A, t_{i,b}^A\})$.

Since only the isoscalar η_2 couples strongly to $SU(3)_C$ gluons through a loop of the color-triplet T_2-fermions (see footnote 3), we have

$$\mathcal{L}_{\eta_T gg} = \sqrt{2}\mathcal{L}_{\eta_{L,H}gg} = \frac{g_C^2}{64\pi^2 F_{\eta_T}}\left[N_1 N_{TC}(N_{TC}-1)\right]\eta_T G_{C,\mu\nu}^\alpha \widetilde{G}_C^{\alpha,\mu\nu}\,. \tag{29}$$

Because of the large numerator, $\mathcal{L}_{\eta_T gg}$ is stronger that the standard H coupling to two gluons.

The nonzero WZW couplings of η_T and π_T^0 to a pair of $SU(2)\otimes U(1)$ bosons are

$$\mathcal{L}_{\eta_T BB} = -\frac{g'^2 N_{TC}}{96\pi^2 F_{\eta_T}}\left[N_2(1+12Y_1^2) - \tfrac{3}{2}N_1(N_{TC}-1)(1+12Y_2^2)\right]\eta_T B_{\mu\nu}\widetilde{B}^{\mu\nu}\,, \quad (30)$$

$$\mathcal{L}_{\eta_T WW} = -\frac{g^2 N_{TC}}{96\pi^2 F_{\eta_T}}\left[N_2 - \tfrac{3}{2}N_1(N_{TC}-1)\right]\eta_T W^a_{\mu\nu}\widetilde{W}^{a,\mu\nu}\,, \quad (31)$$

$$\mathcal{L}_{\eta_T WB} = -\frac{gg' N_{TC}}{96\pi^2 F_{\eta_T}}\left[N_2 - \tfrac{3}{2}N_1(N_{TC}-1)\right]\eta_T W^3_{\mu\nu}\widetilde{B}^{\mu\nu}\,, \quad (32)$$

$$\mathcal{L}_{\pi_T^0 BB} = -\frac{g'^2 N_{TC}}{16\pi^2 F_{\pi}}\left[Y_1\cot\chi - \tfrac{3}{2}(N_{TC}-1)Y_2\tan\chi\right]\pi_T^0 B_{\mu\nu}\widetilde{B}^{\mu\nu}\,, \quad (33)$$

$$\mathcal{L}_{\pi_T^0 WB} = -\frac{gg' N_{TC}}{16\pi^2 F_{\pi}}\left[Y_1\cot\chi - \tfrac{3}{2}(N_{TC}-1)Y_2\tan\chi\right]\pi_T^0 W^3_{\mu\nu}\widetilde{B}^{\mu\nu}\,. \quad (34)$$

From these we obtain

$$\mathcal{L}_{\eta_T\gamma\gamma} = -\frac{e^2 N_{TC}}{32\pi^2 F_{\eta_T}}\left[N_2(1+4Y_1^2) - \tfrac{3}{2}N_1(N_{TC}-1)(1+4Y_2^2)\right]\eta_T F_{\mu\nu}\widetilde{F}^{\mu\nu}\,, \quad (35)$$

$$\mathcal{L}_{\eta_T Z\gamma} = -\frac{e\sqrt{g^2+g'^2}N_{TC}}{32\pi^2 F_{\eta_T}}\Big[N_2(1-2(1+4Y_1^2)\sin^2\theta_W) - \tfrac{3}{2}N_1(N_{TC}-1)(1-2(1+4Y_2^2)\sin^2\theta_W)\Big]\eta_T F_{\mu\nu}\widetilde{Z}^{\mu\nu}\,, \quad (36)$$

$$\mathcal{L}_{\eta_T ZZ} = -\frac{(g^2+g'^2)N_{TC}}{96\pi^2 F_{\eta_T}}\Big\{N_2\left[1-3\sin^2\theta_W+3(1+4Y_1^2)\sin^4\theta_W\right] - \tfrac{3}{2}N_1(N_{TC}-1)\left[1-3\sin^2\theta_W+3(1+4Y_2^2)\sin^4\theta_W\right]\Big\}\eta_T Z_{\mu\nu}\widetilde{Z}^{\mu\nu}\,, \quad (37)$$

$$\mathcal{L}_{\eta_T W^+W^-} = -\frac{g^2 N_{TC}}{48\pi^2 F_{\eta_T}}\left[N_2 - \tfrac{3}{2}N_1(N_{TC}-1)\right]\eta_T W^+_{\mu\nu}\widetilde{W}^{-,\mu\nu}\,, \quad (38)$$

$$\mathcal{L}_{\pi_T^0\gamma\gamma} = -\frac{e^2 N_{TC}}{8\pi^2 F_{\pi}}\left[Y_1\cot\chi - \tfrac{3}{2}(N_{TC}-1)Y_2\tan\chi\right]\pi_T^0 F_{\mu\nu}\widetilde{F}^{\mu\nu}\,, \quad (39)$$

$$\mathcal{L}_{\pi_T^0 Z\gamma} = -\frac{e\sqrt{g^2+g'^2}\,(1-4\sin^2\theta_W)N_{TC}}{16\pi^2 F_{\pi}} \times\left[Y_1\cot\chi - \tfrac{3}{2}(N_{TC}-1)Y_2\tan\chi\right]\pi_T^0 F_{\mu\nu}\widetilde{Z}^{\mu\nu}\,, \quad (40)$$

$$\mathcal{L}_{\pi_T^0 ZZ} = \frac{(g^2+g'^2)\sin^2\theta_W(1-2\sin^2\theta_W)N_{TC}}{16\pi^2 F_{\pi}} \times\left[Y_1\cot\chi - \tfrac{3}{2}(N_{TC}-1)Y_2\tan\chi\right]\pi_T^0 Z_{\mu\nu}\widetilde{Z}^{\mu\nu}\,. \quad (41)$$

Recall that $N_1 = 1$ and $N_2 = 3(N_{TC}-2)$ for the model in Eq. (1) and note that $1+4Y_i^2 = 2(Q_{Ui}^2 + Q_{Di}^2)$, twice the sum of the squares of technifermion T_i's electric charges. Notice also the potential for cancellations between the T_1 and T_2 terms in these expressions that we mentioned above. This will have an especially striking effect on $\sigma B(gg\to\eta_T\to\gamma\gamma)$. A similar cancellation occurs between the $\eta_T\to\gamma\gamma$ and $\pi_T^0\to\gamma\gamma$ amplitudes.

It is clear from these interactions that the rates for $\eta_{L,H} \to ZZ^* \to 4\ell$ and $\eta_{L,H} \to WW^* \to \ell\nu\ell\nu$ are very much less than $\eta_{L,H} \to \gamma\gamma$. The question of whether the ZZ^* and, to a lesser extent, the WW^* data reported by ATLAS and CMS are real or poorly understood backgrounds may be resolved by the data taken in 2012. We will comment on $\eta_{_L} \to Z\gamma$ rate in Sec. 6. Finally, with the complete mixing of Eq. (24), the coupling of $\eta_{L,H}$ to two electroweak bosons V_1 and V_2 is given by

$$\mathcal{L}_{\eta_{L,H}V_1V_2} = \sqrt{\tfrac{1}{2}} \left(\mathcal{L}_{\eta_{_T}V_1V_2} \mp \mathrm{sgn}(b_2)\, \mathcal{L}_{\pi^0_T V_1V_2} \right) . \tag{42}$$

Consider the $\eta_{L,H}\bar{f}f$ couplings now. From Eq. (26), they are determined by the ETC interactions coupling quarks and leptons to technifermions. These are the same interactions responsible for the SM fermions' masses (except for most of m_t) and it is therefore tempting to assume that the couplings to $\bar{f}f$ are simply of order m_f/F_{η_T}. This is naive, however. As discussed in Ref. [18, 55], a generic scenario for the fermions' ETC couplings in a two-scale model is that SM fermions f connect to T_1 and T_1 to T_2. In walking technicolor, the one-loop f–T_1–f graphs and the two-loop f–T_1–T_2–T_1–f graphs can be comparable. Thus, it is not at all obvious that the sum of these two contributions to the $\eta_{_T}$ and π^0_T couplings to $\bar{f}f$ have a simple proportionality to m_f. Therefore, we write

$$\begin{aligned} \mathcal{L}_{\eta_{_T}\bar{f}f} &= i\sum_f \frac{\zeta_{\eta_{_T},f}\, m_f}{F_{\eta_T}} \eta_{_T} \bar{f}\gamma_5 f \,, \\ \mathcal{L}_{\pi^0_T\bar{f}f} &= i\sum_f \frac{\zeta_{\pi_T,f}\, m_f}{F_{\pi}} \pi^0_T \bar{f}\gamma_5 f \,, \end{aligned} \tag{43}$$

where the factors ζ_f for $\eta_{_T}$ and π^0_T will have to be fixed by experiment.[9]

6. $\eta_{L,H}$ Phenomenology

We begin with a comparison of the rates of gg fusion of $\eta_{L,H}$ and the SM Higgs. The coupling of H to two gluons is given to sufficient accuracy by

$$\mathcal{L}_{Hgg} = \frac{g_C^2}{48\pi^2 v} H G^{\alpha}_{C,\mu\nu} G_C^{\alpha,\mu\nu} \,. \tag{44}$$

Then, using $\mathcal{L}_{\eta_{_T}gg}$ from Eq. (29), and assuming the complete mixing of Eq. (24) and $M_{\eta_{L,H}} = M_H$, we have

$$\frac{\sigma(gg \to \eta_{L,H})}{\sigma(gg \to H)} = \left(\frac{3N_1 N_{TC}(N_{TC}-1)v}{4\sqrt{2}F_{\eta_T}} \right)^2 = \frac{40.5}{1+35\sin^2\chi} \,. \tag{45}$$

[9] Actually, there is no reason that these Yukawa interactions should be parity-conserving but, for our purpose here, this assumption is sufficient.

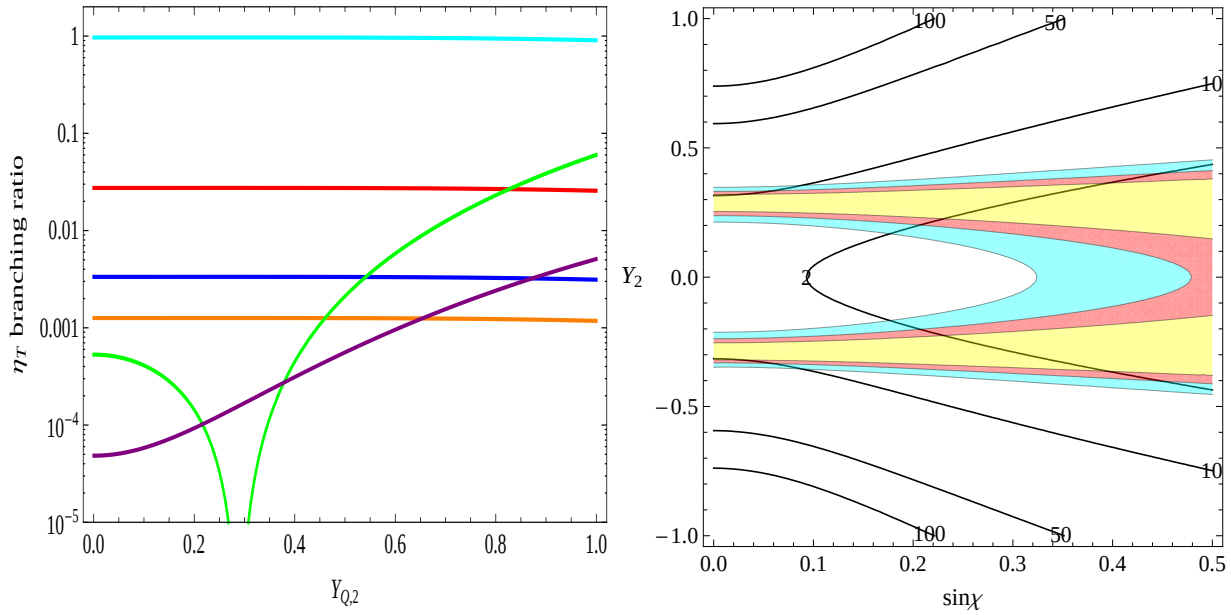

Figure 6: Left: The decay branching ratios as a function of Y_2 for a 125 GeV $\eta_T \to gg$ (teal), $\bar{b}b$ (red), $\tau^+\tau^-$ (blue), $\bar{c}c$ (orange), $\gamma\gamma$ (green) and $Z\gamma$ for a real photon and on-shell Z (purple). The WW^* and ZZ^* rates are negligible. See the text for how $\bar{f}f$ couplings are set. Right: The ratio $R_H = \sigma B(gg \to \eta_L \to \gamma\gamma)/\sigma B(gg \to H \to \gamma\gamma)$ for $M_{\eta_T} = M_H = 125\,\text{GeV}$, as a function of $\sin\chi$ and Y_2. $R_H < 1$ (yellow), $1.0 < R_H < 2.0$ (ochre), $2.0 < R_H < 4.0$ (teal). Overlaid on this plot are contours $\sigma B(gg \to \eta_T \to Z\gamma)/\sigma B(gg \to H \to Z\gamma)$.

The second equality is for $N_{TC} = 4$, $N_1 = 1$ and $N_2 = 6$. If we use the limit $\sin\chi < 0.3$ obtained for LSTC with $M_{\rho_T} \lesssim 300\,\text{GeV}$ [48, 41], this ratio is $\gtrsim 9.8$. This large gg-production rate will be compensated by a $B(\eta_L \to \gamma\gamma)$ that is suppressed by the cancellation mentioned above.

In the rest of this section we present results assuming both zero η_T-π_T^0 mixing and complete mixing. They consist mainly of the $\eta_{L,H}$ decay branching ratios, the ratio $\sigma B(gg \to \eta_L \to \gamma\gamma)/\sigma B(gg \to H \to \gamma\gamma)$ for $M_H = M_{\eta_L} = 125\,\text{GeV}$, and $\sigma B(gg \to \eta_H \to \gamma\gamma)$ versus the η_L-rate. The last assumes $M_{\eta_H} = 180\,\text{GeV}$, a value corresponding to complete η_T-π_T^0 mixing at $M_{\pi_T^\pm} = 155\,\text{GeV}$. We assume throughout that the T_1 hypercharge $Y_1 = 0$, which is strongly suggested by the absence of a signal for $\omega_T \to \ell^+\ell^-$ at the rate expected in LSTC for $M_{\omega_T} \simeq 300\,\text{GeV}$ [56]. The value $\sin\chi = 0.3$ is used to determine F_{η_T} and the π_T^0 couplings in the branching-ratio plots; it is varied for calculating the branching ratios in the σB plots. We assume ζ_τ and ζ_b factors that give the same σB as the SM Higgs.[10]

[10] In more detail: For a specific η_T-π_T^0 mixing, we calculate ζ_f with $Y_1 = Y_2 = 0$. (There is only weak dependence on Y_2.) Solving $\sigma B(gg \to \eta_L \to \bar{f}f)/(\sigma B(gg \to H \to \bar{f}f) = 1$ for ζ_τ and ζ_b, and taking all ζ_f equal the larger of the two, gives ζ_f as a function of $\sin\chi$ for each η_T-π_T^0 mixing. The results presented here for gauge boson pair-production rates (mostly diphoton) are insensitive to ζ_f so long as $B(\eta_L \to \bar{f}f) \lesssim B(H \to \bar{f}f)$ because the η_T width is dominated by its gg-decay rate.

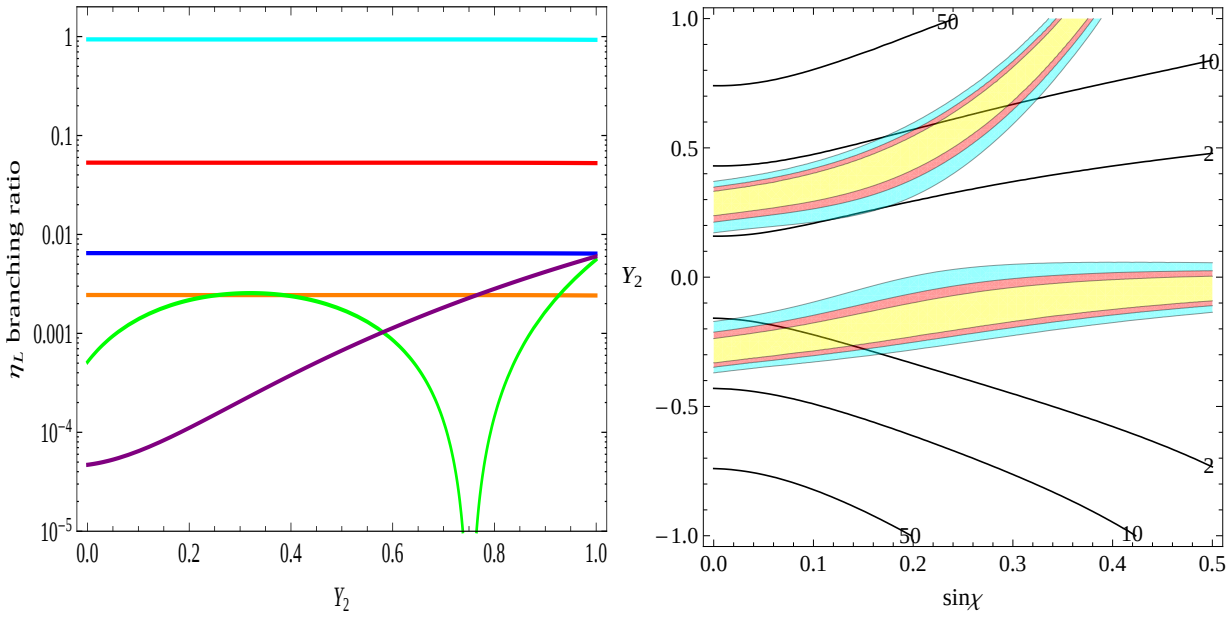

Figure 7: Left: The decay branching ratios as a function of Y_2 for a 125 GeV $\eta_{_L} \to gg$ for the case of complete $\eta_{_T}$-$\pi^0_{_T}$ mixing with $\mathrm{sgn}(b_2) > 0$. Right: The ratio $R_H = \sigma B(gg \to \eta_{_L} \to \gamma\gamma)/\sigma B(gg \to H \to \gamma\gamma)$ for $M_H = M_{\eta_{_L}} = 125\,\mathrm{GeV}$, as a function of $\sin\chi$ and Y_2. Overlaid on this plot are contours $\sigma B(gg \to \eta_{_L} \to Z\gamma)/\sigma B(gg \to H \to Z\gamma)$. The color codes are as in Fig. 6.

The $\eta_{_T}$ branching ratios and $\gamma\gamma$ production rate are shown in Fig. 6 for the case of no mixing with $\pi^0_{_T}$. For $Y_1 = 0$, these are even functions of Y_2. As anticipated, the zero in the $\gamma\gamma$ rate at $Y_2 = 0.29$ is due to a cancellation between the T_1 and T_2 contributions. For $\sin\chi < 0.3$, there are narrow bands ($\Delta Y_2 \simeq 0.07$) centered on $Y_2 = \pm 0.29$ where the $\eta_{_T} \to \gamma\gamma$ rate is up to four times as large as the SM Higgs rate. We expect that any additional jets associated with this gg-production would be color-connected with the primary production and not exhibit a rapidity gap. To our knowledge, there is no published analysis of this. Contours giving the ratio $\sigma B(gg \to \eta_{_T} \to Z\gamma)/\sigma B(gg \to H \to Z\gamma)$ are overlaid on this plot. The ratio is 2–10 for $\sin\chi < 0.3$. We have estimated the rate for $\eta_{_T} \to Z\gamma^* \to 4\ell$ and found that, for a luminosity of $10\,\mathrm{fb}^{-1}$, at most half an event would have been produced. After efficiencies, essentially none of the events in Figs. 2, 4 could be due to this $\eta_{_T}$ decay.

The $\eta_{_L}$ branching ratios and $\gamma\gamma$ rate compared to the SM Higgs are shown for the complete-mixing cases and $Y_1 = 0$ in Fig. 7 for $\mathrm{sgn}(b_2) > 0$ and Fig. 8 for $\mathrm{sgn}(b_2) < 0$. These two cases go into each other by reversing the signs of Y_1 and Y_2. For $Y_1 = 0$ and $\sin\chi = 0.3$, the zero in $B(\eta_{_L} \to \gamma\gamma)$ for $Y_2 > 0$ occurs for the two cases at 0.75 and 0.11, respectively. Note that $\eta_{_L}$ decay rates are dominated by those for $\eta_{_T}$, in particular $B(\eta_{_L} \to gg) \simeq 100\% \gg B(\eta_{_T} \to \bar{f}f)$. Still, as explained in footnote 10, we have chosen $\eta_{_L}$ couplings to fermions so that $\sigma(gg \to \eta_{_L} \to \bar{b}b \text{ or } \tau^+\tau^-)/\sigma(gg \to H \to \bar{b}b \text{ or } \tau^+\tau^-) \sim 1$. The allowed ranges of $\sigma B(\eta_{_L} \to \gamma\gamma)$ occur in bands of thickness $\Delta Y_2 \simeq 0.2$ and, for the two

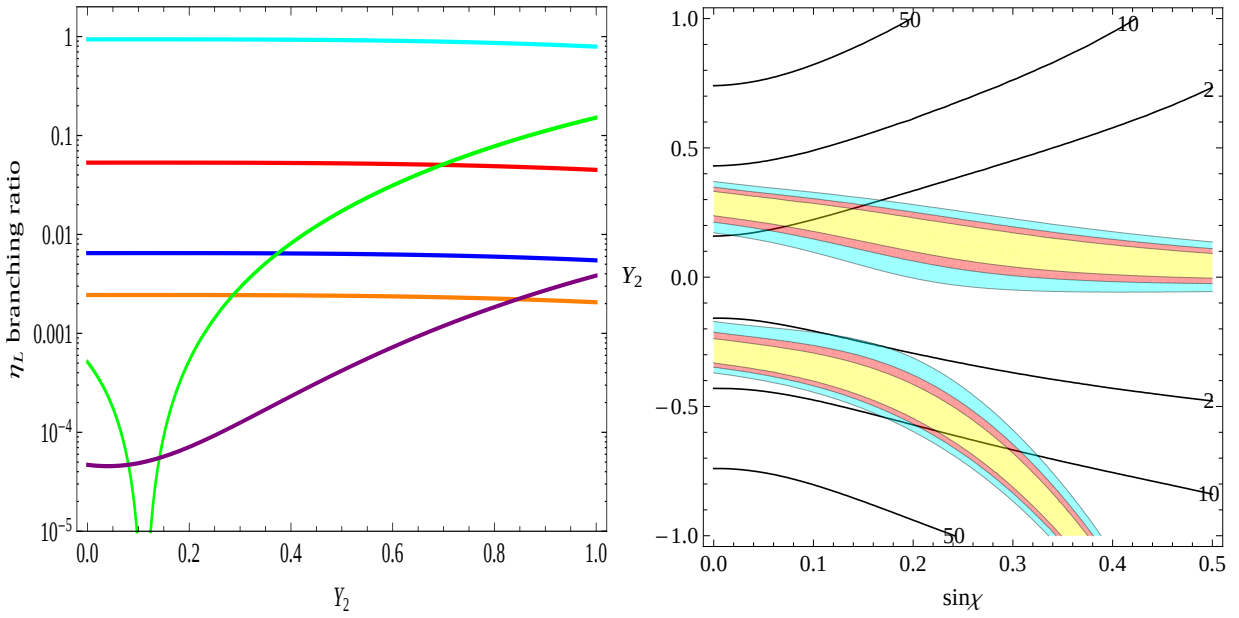

Figure 8: Left: The decay branching ratios as a function of Y_2 for a 125 GeV $\eta_{_L} \to gg$ for the case of complete $\eta_{_T}$-π^0_T mixing with $\mathrm{sgn}(b_2) < 0$. Right: The ratio $R_H = \sigma B(gg \to \eta_{_L} \to \gamma\gamma)/\sigma B(gg \to H \to \gamma\gamma)$ for $M_H = M_{\eta_{_L}} = 125\,\mathrm{GeV}$, as a function of $\sin\chi$ and Y_2. Overlaid on this plot are contours $\sigma B(gg \to \eta_{_L} \to Z\gamma)/\sigma B(gg \to H \to Z\gamma)$. The color codes are as in Fig. 6.

mixing cases, they are mirror reflections of each other about $Y_2 = 0$ for $Y_1 = 0$. In these allowed regions, $B(\eta_{_L} \to \gamma\gamma)$ is 4–10 times smaller than the SM Higgs branching ratio. As in the unmixed case, the $\eta_{_L} \to Z\gamma$ rate is 2–10 times the SM Higgs rate, much too small to account for the data in Figs. 2,4.

Finally, in Fig. 9 we overlay the $\sigma B(gg \to \eta_{_L} \to \gamma\gamma)/\sigma B(gg \to H \to \gamma\gamma)$ ratios with contours of $\sigma B(gg \to \eta_{_H} \to \gamma\gamma)$ given in picobarns. Based on a CMS search for diphoton resonances in $2.2\,\mathrm{fb}^{-1}$ of 7-TeV data [57], we estimate that $\sigma B(gg \to \eta_{_H} \to \gamma\gamma) \lesssim 0.25\,\mathrm{pb}$ is allowed. This is consistent with both branches of the green-shaded region of this figure for $|Y_2| < 0.4$.

7. $\eta_{_T}$-π^0_T Mixing and LSTC Collider Phenomenology

The discussion in this section is based on our interpretation of CDF's dijet excess as the production of a 280–290 GeV ρ_T which decays to a 150–160 GeV π_T plus a W-boson [39, 51, 40, 41].[11] The π_T decays 90–95% of the time to $\bar{q}q$ jets (which may or may not contain b-jets, hence the spread we assume in M_{π_T} and M_{ρ_T}). With large $\eta_{_T}$-π^0_T mixing, the $\rho^\pm_T \to W\pi^0_T$

[11] In Ref. [40] we found that $\simeq 25\%$ of the Tevatron signal was due to $a_T \to W\pi_T$, with $M_{a_T} = 1.1 M_{\rho_T}$ assumed.

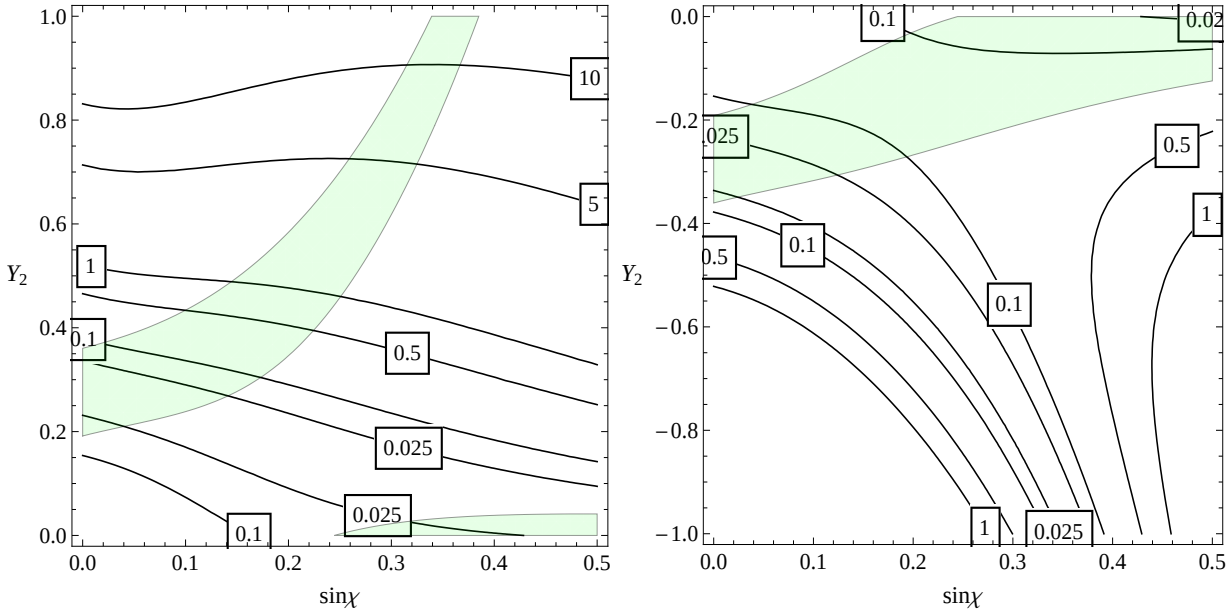

Figure 9: The green-shaded regions are $R_H = \sigma B(gg \to \eta_{_L} \to \gamma\gamma)/\sigma B(gg \to H \to \gamma\gamma) < 4$ for $M_H = M_{\eta_{_L}} = 125\,\mathrm{GeV}$ and $\mathrm{sgn}(b_2) > 0$, as a function of $\sin\chi$ and Y_2. Overlaid on these plots are contours $\sigma B(gg \to \eta_{_H} \to \gamma\gamma)$, in picobarns, for $M_{\eta_{_H}} = 180\mathrm{GeV}$.

component of the 150 GeV dijet signal is absent. To some extent, this loss is replaced by $\rho_T \to W\eta_{_L} \to \ell^\pm\nu jj$ with $M_{jj} \simeq 125\,\mathrm{GeV}$. Since this decay is dominated by its $\rho_T \to W\pi_T^0$ component, the dijets are mainly $\bar{q}q$ jets. Detailed calculation of this new phenomenology requires either a complete rewrite of the PYTHIA code for LSTC or a new implementation in another amplitude generator because changes in the ρ_T partial widths make it difficult to guess individual production rates. This is beyond the scope of this paper. Here we will be satisfied with a list of the important changes we anticipate.

1) The rate for $\rho_T, a_T \to W\pi_T$ is likely to be reduced. Simply (and naively) eliminating the $W\pi_T^0$ mode results in about a 35% reduction of the dijet excess signal [40].

2) There will be a $\rho_T, a_T \to W\eta_{_L} \to \ell\nu jj$ signal at $M_{jj} \simeq 125\,\mathrm{GeV}$, largely due to its $W\pi_T^0$ component. The dijet peak may overlap somewhat with the $\rho_T^0 \to W^\pm\pi_T^\mp$ dijet excess. While $\rho_T, a_T \to W\eta_{_L}$ is suppressed by the mixing, it is enhanced by the greater phase space and, so, may not be much smaller that the $W^\pm\pi_T^\mp$ rate. Note that this will appear as associated production of $\eta_{_L}$ with W, but the Wjj invariant mass will peak near M_{ρ_T}. There is *no* significant associated production of $\eta_{_L}$ with Z.

3) The channel $\rho_T^\pm \to \pi_T^\pm\eta_{_L}$ is open and the π_T^0 component of this amplitude is a strong process, unsuppressed by $\sin\chi$. Even though the Q-value for this decay is only $\sim 5\,\mathrm{GeV}$, this mode could be an important part of the $\rho_T^\pm$ width and its production rate

might be as large $\sim 500\,\text{fb}$ at the LHC. We do not know of any limit on this four-jet process, especially since the two dijets have rather different masses.

4) A primary signal at the LHC for confirming the CDF dijet excess is $\rho_T^\pm \to Z\pi_T^\pm \to \ell^+\ell^- jj$. In Ref. [41], we predicted a rate of 190 fb for this final state (220 fb for $Y_1 = 0$ and $\sin\chi = 0.3$). This rate is likely reduced by the open $\pi_T^\pm \eta_{_L}$ channel; a *rough* estimate is a 50–60% reduction. This is an unfortunate hit to an otherwise very promising channel for the 2012 data.

5) A similar reduction in the rate for $\rho_T^\pm \to WZ \to 3\ell\nu$ or $\ell^+\ell^- jj$ is to be expected. This would weaken the bound $\sin\chi < 0.3$ implied by the recent CMS data [48]. On the other hand, the idea of low-scale TC does not make much sense if $\sin\chi \gtrsim \frac{1}{2}$.

6) Last, though not least, we again urge a search for $\eta_{_H} \to \gamma\gamma$ near 180 GeV. Over most of the allowed regions in Fig. 9, $\sigma B(\eta_{_H} \to \gamma\gamma) \lesssim 0.25\,\text{pb}$ at the LHC. The upper end of this range should be accessible soon—if not already excluded.

8. Conclusions

The "Higgs impostor" proposal made in this paper is motivated both by our desire for a technicolor explanation for the new boson $X(125)$ and by the apparent differences between the ATLAS and/or CMS data and what is expected for a Higgs boson. The most important discrepancy is the $ZZ^* \to 4\ell$ data of both experiments, a channel valued for its high mass resolution. The low number of what might be called "gold-plated" events in the CMS data — those which appear to contain a real, on-shell Z-boson and which fall in the dark "signal region" of the three distributions, M_{Z1} and M_{Z2} versus each other and $M_{4\ell}$ — is one glaring example. The ATLAS $ZZ^* \to 4\ell$ data appears to have a similar deficit of gold-plated events. A second example is the rather large fluctuations in the number of events in the signal region of M_{Z1} vs. M_{Z2} between the July and November/December 2012 data releases by both experiments. All this may just be statistics at work and be resolved in favor of the popular Higgs description when the next large batch of data is released. But, as we said at the outset, the SM Higgs outcome would confront theorists anew with the thorny questions of naturalness, hierarchy and flavor. If, on the other hand, the discrepancies in the data are real, then we may, at long last, have begun to unravel the mystery of electroweak symmetry breaking. That is a lot to hope for.

In this paper we proposed an alternative to the SM Higgs interpretation: $X(125)$ is a technipion, $\eta_{_L}$. Our proposal has several immediately testable consequences in addition to discrediting the $X \to ZZ^*, WW^*$ data. Chief among these is that there is likely to be another Higgs impostor state $\eta_{_H}$ which is not far from 200 GeV and which may be visible in the diphoton spectrum. If the CDF dijet excess is real, and our LSTC interpretation of it correct, then $M_{\eta_{_H}} = 170$–$190\,\text{GeV}$. Furthermore, the M_{jj} spectrum in the range ~ 100–$150\,\text{GeV}$ range is contaminated by a sizable $\rho_T \to W\eta_{_L}$ component that will complicate

modeling in terms of standard diboson production as done, e.g., by CMS in Ref [58]. Finally, if all this is correct, we expect the LSTC phenomenology presented in Ref. [41] to be modified substantially.

Acknowledgments

We are grateful to T. Appelquist, W. Bardeen, K. Black, T. Bose, P. Catastini, A. DeRoeck, C. Fantasia, C. Hill, K. Terashi, B. Zhou and J. Zhu for valuable conversations and advice. This work was supported by Fermilab operated by Fermi Research Alliance, LLC, U.S. Department of Energy Contract DE-AC02-07CH11359 (EE and AM) and in part by the U.S. Department of Energy under Grant DE-FG02-91ER40676 (KL). KL's research was also supported in part by Laboratoire d'Annecy-le-Vieux de Physique Theorique (LAPTh) and the CERN Theory Group and he thanks LAPTh and CERN for their hospitality.

References

[1] **ATLAS** Collaboration, G. Aad *et. al.*, "Observation of a new particle in the search for the Standard Model Higgs boson with the ATLAS detector at the LHC," *Phys.Lett.* **B716** (2012) 1–29, 1207.7214.

[2] **CMS** Collaboration, S. Chatrchyan *et. al.*, "Observation of a new boson at a mass of 125 GeV with the CMS experiment at the LHC," *Phys.Lett.* **B716** (2012) 30–61, 1207.7235.

[3] S. Glashow, "Partial Symmetries of Weak Interactions," *Nucl.Phys.* **22** (1961) 579–588.

[4] S. Weinberg, "A Model of Leptons," *Phys.Rev.Lett.* **19** (1967) 1264–1266.

[5] A. Salam, "Weak and Electromagnetic Interactions," *Conf.Proc.* **C680519** (1968) 367–377.

[6] F. Englert and R. Brout, "Broken Symmetry and the Mass of Gauge Vector Mesons," *Phys.Rev.Lett.* **13** (1964) 321–323.

[7] P. W. Higgs, "Broken symmetries, massless particles and gauge fields," *Phys.Lett.* **12** (1964) 132–133.

[8] G. Guralnik, C. Hagen, and T. Kibble, "Global Conservation Laws and Massless Particles," *Phys.Rev.Lett.* **13** (1964) 585–587.

[9] **CMS** Collaboration, "Combination of standard model Higgs boson searches and measurements of the properties of the new boson with a mass near 125 GeV,". CMS PAS Hig-12-045.

[10] **CMS** Collaboration https://twiki.cern.ch/twiki/bin/view/CMSPublic/Hig12045TWiki, 2012.

[11] **ATLAS** Collaboration, "An update of combined measurements of the new Higgs-like boson with high mass resolution channels," Tech. Rep. ATLAS-CONF-2012-170, CERN, Geneva, Dec, 2012.

[12] **ATLAS** Collaboration, "Observation of an excess of events in the search for the Standard Model Higgs boson in the H ZZ() 4l channel with the ATLAS detector," Tech. Rep. ATLAS-CONF-2012-169, CERN, Geneva, Dec, 2012.

[13] **CMS** Collaboration, "Latest on the Higgs from CMS, C. Paus at HCP, Kyoto." Nov., 2012.

[14] **ATLAS** Collaboration, "ATLAS Status Report on SM Higgs Search/Measurements, K. Einsweiler at HCP, Kyoto." Nov., 2012.

[15] L. Susskind, "Dynamics of Spontaneous Symmetry Breaking in the Weinberg-Salam Theory," *Phys.Rev.* **D20** (1979) 2619–2625.

[16] G. 't Hooft, "Naturalness, chiral symmetry, and spontaneous chiral symmetry breaking," *NATO Adv.Study Inst.Ser.B Phys.* **59** (1980) 135.

[17] S. Weinberg, "Implications of Dynamical Symmetry Breaking: An Addendum," *Phys.Rev.* **D19** (1979) 1277–1280.

[18] K. D. Lane and E. Eichten, "Two Scale Technicolor," *Phys. Lett.* **B222** (1989) 274.

[19] K. Lane and A. Martin, "An Effective Lagrangian for Low-Scale Technicolor," *Phys. Rev.* **D80** (2009) 115001, 0907.3737.

[20] A. Delgado, K. Lane, and A. Martin, "A Light Scalar in Low-Scale Technicolor," *Phys.Lett.* **B696** (2011) 482–486, 1011.0745.

[21] K. Cheung and T.-C. Yuan, "Could the excess seen at 124-126 GeV be due to the Randall-Sundrum Radion?," *Phys.Rev.Lett.* **108** (2012) 141602, 1112.4146.

[22] S. Matsuzaki and K. Yamawaki, "Techni-dilaton at 125 GeV," *Phys.Rev.* **D85** (2012) 095020, 1201.4722.

[23] S. Matsuzaki and K. Yamawaki, "Discovering 125 GeV techni-dilaton at LHC," 1206.6703.

[24] D. D. Dietrich, F. Sannino, and K. Tuominen, "Light composite Higgs from higher representations versus electroweak precision measurements: Predictions for LHC," *Phys. Rev.* **D72** (2005) 055001, hep-ph/0505059.

[25] D. Elander and M. Piai, "The decay constant of the holographic techni-dilaton and the 125 GeV boson," 1208.0546.

[26] Z. Chacko, R. Franceschini, and R. K. Mishra, "Resonance at 125 GeV: Higgs or Dilaton/Radion?," 1209.3259.

[27] B. Bellazzini, C. Csaki, J. Hubisz, J. Serra, and J. Terning, "A Higgslike Dilaton," 1209.3299.

[28] W. D. Goldberger, B. Grinstein, and W. Skiba, "Distinguishing the Higgs boson from the dilaton at the Large Hadron Collider," *Phys.Rev.Lett.* **100** (2008) 111802, 0708.1463.

[29] I. Low, J. Lykken, and G. Shaughnessy, "Singlet scalars as Higgs imposters at the Large Hadron Collider," *Phys.Rev.* **D84** (2011) 035027, 1105.4587.

[30] G. Burdman, C. E. Haluch, and R. D. Matheus, "Is the LHC Observing the Pseudo-scalar State of a Two-Higgs Doublet Model ?," *Phys.Rev.* **D85** (2012) 095016, 1112.3961.

[31] B. Holdom, "A pseudoscalar at the LHC: technicolor vs a fourth family," *Phys.Lett.* **B709** (2012) 381–384, 1201.0185.

[32] I. Low, J. Lykken, and G. Shaughnessy, "Have We Observed the Higgs (Imposter)?," 1207.1093.

[33] R. S. Chivukula, B. Coleppa, P. Ittisamai, H. E. Logan, A. Martin, *et. al.*, "Discovering Strong Top Dynamics at the LHC," 1207.0450.

[34] B. Coleppa, K. Kumar, and H. E. Logan, "Can the 126 GeV boson be a pseudoscalar?," 1208.2692.

[35] M. T. Frandsen and F. Sannino, "Discovering a Light Scalar or Pseudoscalar at The Large Hadron Collider," 1203.3988.

[36] **CMS** Collaboration, J. Incandela, "Status of the CMS SM Higgs Search, July 4, 2012,".

[37] J. Wess and B. Zumino, "Consequences of anomalous Ward identities," *Phys. Lett.* **B37** (1971) 95.

[38] E. Witten, "Global Aspects of Current Algebra," *Nucl. Phys.* **B223** (1983) 422–432.

[39] **CDF** Collaboration, T. Aaltonen *et. al.*, "Invariant Mass Distribution of Jet Pairs Produced in Association with a W boson in ppbar Collisions at sqrt(s) = 1.96 TeV," *Phys. Rev. Lett.* **106** (2011) 171801, 1104.0699.

[40] E. J. Eichten, K. Lane, and A. Martin, "Technicolor Explanation for the CDF W_{jj} Excess," *Phys.Rev.Lett.* **106** (2011) 251803, 1104.0976.

[41] E. Eichten, K. Lane, A. Martin, and E. Pilon, "Testing the Technicolor Interpretation of the CDF Dijet Excess at the 8-TeV LHC," 1206.0186.

[42] **CMS** Collaboration https://twiki.cern.ch/twiki/bin/view/CMSPublic/Hig12041TWiki#4l_plots, 2012.

[43] **CMS** Collaboration, S. Chatrchyan *et. al.*, "On the mass and spin-parity of the Higgs boson candidate via its decays to Z boson pairs," 1212.6639.

[44] **CDF, D0** Collaboration, T. Aaltonen *et. al.*, "Evidence for a particle produced in association with weak bosons and decaying to a bottom-antibottom quark pair in Higgs boson searches at the Tevatron," 1207.6436.

[45] **CDF** Collaboration, T. Aaltonen *et. al.*, "Search for the standard model Higgs boson decaying to a $b\bar{b}$ pair in events with no charged leptons and large missing transverse energy using the full CDF data set," *Phys.Rev.Lett.* **109** (2012) 111805, 1207.1711.

[46] A. G. Cohen and H. Georgi, "WALKING BEYOND THE RAINBOW," *Nucl. Phys.* **B314** (1989) 7.

[47] C. T. Hill, "Topcolor assisted technicolor," *Phys. Lett.* **B345** (1995) 483–489, hep-ph/9411426.

[48] **CMS** Collaboration, S. Chatrchyan *et. al.*, "Search for exotic particles decaying to WZ in pp collisions at sqrt(s)=7 TeV," 1206.0433.

[49] E. Eichten and K. D. Lane, "Dynamical Breaking of Weak Interaction Symmetries," *Phys. Lett.* **B90** (1980) 125–130.

[50] K. Lane and S. Mrenna, "The collider phenomenology of technihadrons in the technicolor Straw Man Model," *Phys. Rev.* **D67** (2003) 115011, hep-ph/0210299.

[51] **CDF** Collaboration http://www-cdf.fnal.gov/physics/ewk/2011/wjj/7_3.html.

[52] R. F. Dashen, "Chiral SU(3) x SU(3) as a symmetry of the strong interactions," *Phys. Rev.* **183** (1969) 1245–1260.

[53] T. Sjostrand, S. Mrenna, and P. Z. Skands, "PYTHIA 6.4 Physics and Manual," *JHEP* **0605** (2006) 026, hep-ph/0603175.

[54] J. A. Harvey, C. T. Hill, and R. J. Hill, "Standard Model Gauging of the Wess-Zumino-Witten Term: Anomalies, Global Currents and pseudo-Chern-Simons Interactions," *Phys. Rev.* **D77** (2008) 085017, 0712.1230.

[55] K. D. Lane and M. V. Ramana, "Walking technicolor signatures at hadron colliders," *Phys. Rev.* **D44** (1991) 2678–2700.

[56] **ATLAS** Collaboration, G. Aad *et. al.*, "Search for high-mass resonances decaying to dilepton final states in pp collisions at a center-of-mass energy of 7 TeV with the ATLAS detector," 1209.2535.

[57] **CMS** Collaboration, S. Chatrchyan *et. al.*, "Search for signatures of extra dimensions in the diphoton mass spectrum at the Large Hadron Collider," 1112.0688.

[58] **CMS** Collaboration, S. Chatrchyan *et. al.*, "Study of the dijet mass spectrum in $pp \to W+$ jets events at $\sqrt{s} = 7$ TeV," 1208.3477.